Stem Cell Reports
Article
OPEN ACCESS

Identification of a Multipotent Self-Renewing Stromal Progenitor Population during Mammalian Kidney Organogenesis

Akio Kobayashi,[1,2,3,5,*] Joshua W. Mugford,[1] A. Michaela Krautzberger,[1,4] Natalie Naiman,[2] Jessica Liao,[2] and Andrew P. McMahon[1,3,4]

[1]Department of Stem Cell and Regenerative Biology, Harvard University, 7 Divinity Avenue, Cambridge, MA 02138, USA
[2]Renal Division, Department of Medicine, Brigham and Women's Hospital, Harvard Medical School, 4 Blackfan Circle, Boston, MA 02115, USA
[3]Harvard Stem Cell Institute, 1350 Massachusetts Avenue, Cambridge, MA 02138, USA
[4]Department of Stem Cell Biology and Regenerative Medicine, Eli and Edythe Broad Center for Regenerative Medicine and Stem Cell Research, W. M. Keck School of Medicine, University of Southern California, Los Angeles, 1425 San Pablo Street, Los Angeles, CA 90089, USA
[5]Present address: Division of Nephrology, Institute for Stem Cell and Regenerative Medicine, University of Washington, 750 Republican Street, Seattle, WA 98040, USA
*Correspondence: akiok@uw.edu
http://dx.doi.org/10.1016/j.stemcr.2014.08.008

SUMMARY

The mammalian kidney is a complex organ consisting of multiple cell types. We previously showed that the *Six2*-expressing cap mesenchyme is a multipotent self-renewing progenitor population for the main body of the nephron, the basic functional unit of the kidney. However, the cellular mechanisms establishing stromal tissues are less clear. We demonstrate that the *Foxd1*-expressing cortical stroma represents a distinct multipotent self-renewing progenitor population that gives rise to stromal tissues of the interstitium, mesangium, and pericytes throughout kidney organogenesis. Fate map analysis of *Foxd1*-expressing cells demonstrates that a small subset of these cells contributes to *Six2*-expressing cells at the early stage of kidney outgrowth. Thereafter, there appears to be a strict nephron and stromal lineage boundary derived from *Six2*-expressing and *Foxd1*-expressing cell types, respectively. Taken together, our observations suggest that distinct multipotent self-renewing progenitor populations coordinate cellular differentiation of the nephron epithelium and renal stroma during mammalian kidney organogenesis.

INTRODUCTION

The kidney contains multiple specialized cell types that have district physiological functions. During embryogenesis, the urogenital system, including the kidney, is derived from the intermediate mesoderm of the developing embryo (Herzlinger, 1995; Saxen, 1987). Formation of the definitive kidney or metanephros in mammals is initiated by reciprocal interactions between two tissues types, the ureteric bud and metanephric mesenchyme, starting around 10.5 days postcoitum (dpc) in the mouse (Costantini and Kopan, 2010; Dressler, 2009; Little and McMahon, 2012; Schedl, 2007). At this time, analysis of transcription factor expression distinguishes two morphologically distinct populations: a core of *Six2*-expressing (*Six2*+) mesenchyme, and an outer layer of *Foxd1*+ cells that likely emerge from a common *Osr1*+ mesenchymal progenitor (Kobayashi et al., 2008; Levinson and Mendelsohn, 2003; Mugford et al., 2008). As the outgrowing ureteric bud enters this mesenchyme and branches, *Six2*+ cells condense around the bud tip forming the cap mesenchyme, whereas *Foxd1*+ cortical stromal cells make up the renal capsule and nephrogenic interstitium between the *Six2*+ population and the outermost connective tissue (the presumptive renal fascia or Gerota's fascia) that surrounds the kidney and adrenal gland (Costantini, 2006; Kobayashi et al., 2008; Levinson et al., 2005).

The *Six2*+ cap mesenchyme is a multipotent self-renewing nephron progenitor population (Kobayashi et al., 2008). In conjunction with ureteric branching, a ureteric epithelium-derived WNT9B signal induces a pathway of nephrogenesis within a subset of *Six2*+ progenitors (Carroll et al., 2005; Karner et al., 2011; Park et al., 2007, 2012). Induced cells undergo an initial aggregation to form the pretubular aggregate. Subsequently, through a mesenchymal-to-epithelial transition, the pretubular aggregate transitions to the renal vesicle that undergoes a series of morphological transformations and patterning processes generating the main body of the nephron from the proximal glomerulus to the distal connecting segment.

The mature nephron, and its accompanying vascular network, is embedded within the cortical and medullary interstitium (Little et al., 2007). This comprises pericytes and mesangial cell types that are intimately associated with the general kidney vasculature and the specialized vasculature of the glomerular capillary loops, respectively (Quaggin and Kreidberg, 2008; Wiggins, 2007), and interstitial fibroblast-like cells that are most prevalent within medullary regions of the mature kidney. Currently, the origins and interrelationships among these cell types are unclear, and the precise role of these stromal components in development, normal kidney function, and disease is poorly understood.

In this study, we have determined the fate map of the *Foxd1*+ cortical stromal cells during kidney development

in vivo in the mouse. These studies demonstrate that the *Foxd1*+ cortical stroma is a multipotent self-renewing progenitor population for stromal cells in the kidney, giving rise to cortical and medullary interstitial cells, mesangial cells, and pericytes of the kidney. Interestingly, *Foxd1*+ stromal progenitors and *Six2*+ nephron progenitors form two mutually exclusive progenitor compartments shortly after the onset of ureteric branching. Prior to this stage, we observed a small but significant contribution of *Foxd1*+ cells to the *Six2*+ progenitor population. Our observations also suggest that the *Foxd1*+ stromal progenitor and *Six2*+ nephron progenitor populations temporally and spatially coordinate cellular differentiation. These data highlight the roles of distinct progenitor compartments in the assembly of the mammalian kidney.

RESULTS

Generation of *Foxd1-Cre* Knockin Mouse Alleles

During early stages of kidney development, *Foxd1* is specifically expressed in the cortical stroma of the nephrogenic zone (Das et al., 2013; Hatini et al., 1996; Levinson et al., 2005). To determine the fate map of this *Foxd1*-expressing (*Foxd1*+) population, we generated three *Foxd1-Cre* knockin alleles in the mouse, where e*GFPCre* ($Foxd1^{GC/+}$), *eGFPCreER*^{T2} ($Foxd1^{GCE/+}$), and *CreER*^{T2} ($Foxd1^{CE/+}$) transgenes were introduced into the 5′ UTR of the endogenous *Foxd1* locus (Figure S1 available online). These *Foxd1*-Cre knockin alleles ablate *Foxd1* function; however, mice heterozygous for these and previously described null alleles are phenotypically normal and fertile (Hatini et al., 1996; Levinson et al., 2005) (data not shown). The *GCE* and *CE* alleles allow tamoxifen-dependent regulation of Cre recombinase activity (Indra et al., 1999; Kobayashi et al., 2008).

To validate transgene expression patterns of the *Foxd1-Cre* knockin alleles, we examined GFP expression in the developing kidney of $Foxd1^{GC/+}$ and $Foxd1^{GCE/+}$ embryos. In both lines, GFP expression was observed in the cortical stroma during kidney development (Figure S2; data not shown). The nuclear FOXD1 protein colocalized with nuclear GFP in $Foxd1^{GC/+}$ kidneys (Figure S2I), whereas FOXD1 was surrounded by cytoplasmic GFP in $Foxd1^{GCE/+}$ kidneys (Figure S2J). These observations confirmed GFP expression in FOXD1+ cortical stromal cells in the *Foxd1-GC* and *Foxd1-GCE* alleles.

Genome-wide gene expression projects (GenePaint and GUDMAP) have documented *Foxd1* expression in the glomerulus at a low level at 14.5 dpc and at a higher level at 19.5 dpc (Figures S3A and S3B) (Harding et al., 2011; Visel et al., 2004), and microarray analysis suggests podocytes as the likely cell source (Brunskill et al., 2011). Although *Foxd1* mRNA appears to be expressed in most podocytes of maturing-stage glomeruli (Figures S3A and S3B), a recent study showed that Cre recombination was observed only in a subset of podocytes in *Foxd1-eGFPCre* mice during kidney development (Boyle et al., 2014), indicating posttranscriptional regulation for *Foxd1* expression or different sensitivity of detection methods. Consistent with these findings, we detected expression of GFP and FOXD1 in a subset of both podocytes and parietal epithelial cells of maturing-stage glomeruli, but not in less-differentiated capillary loop-stage glomeruli, in the $Foxd1^{GC/+}$ kidney at 15.5 and 18.5 dpc (Figure S3B and S3C; data not shown). We observed *Foxd1-GFP* expression only in the cortical stroma, the visceral (podocytes), and the parietal epithelial cells of the glomerulus. No *Foxd1-GFP* expression was observed in any other tissues of the developing kidney. Thus, the *Foxd1-Cre* knockin alleles faithfully document endogenous FOXD1 expression.

Foxd1+ Cells within the Cortical Stroma Show a Distinct Fate Map to that of *Six2*+ Nephron Progenitors in the Cap Mesenchyme

The fate map of the *Foxd1*+ cortical stroma was compared to that of the *Six2*+ cap mesenchyme. $Foxd1^{GC/+}$ and *Six2-tetoff-eGFPCre* ($Six2^{TGC/+}$) (Kobayashi et al., 2008) mice were intercrossed with mice carrying a *R26R-lacZ* reporter allele ($R26R^{lacZ/+}$) (Soriano, 1999) to permanently label descendant cells from the *Foxd1*+ cortical stromal and *Six2*+ cap mesenchymal cells by β-galactosidase (β-gal) expression.

As expected from our previous study (Kobayashi et al., 2008), analysis of $Six2^{TGC/+}$; $R26R^{lacZ/+}$ kidneys at 14.5 dpc showed β-gal activity confined to the cap mesenchyme and all nephron epithelia including the renal vesicle, S-shaped body, nephron tubule, and visceral and parietal epithelia of the glomerulus (Figures 1A, 1C, and 1E). In striking contrast, $Foxd1^{GC/+}$; $R26R^{lacZ/+}$ displayed a reciprocal pattern of β-gal activity restricted to the cortical stroma, cortical and medullary interstitium, and the glomerular mesangium region (Figures 1B, 1D, and 1F). At later stages, we also observed β-gal activity within podocytes of glomeruli at the maturing stage consistent with *Foxd1* expression within this population (Figures S4A and S4C). A low-variable incomplete β-gal activity was observed in a subset of nephrons (Figures 1D and S4E). Taken together, our observations suggest that the fate maps of *Six2*+ cap mesenchyme and *Foxd1*+ cortical stroma are largely distinct: the former contributing to nephron epithelial cells, and the latter to renal stromal cell types.

The low contribution of *Foxd1*+ descendant cells to regions of the nephron epithelium, normally populated only by cells originating from the *Six2*+ cap mesenchyme, outside of the *Foxd1*+ visceral and parietal epithelia

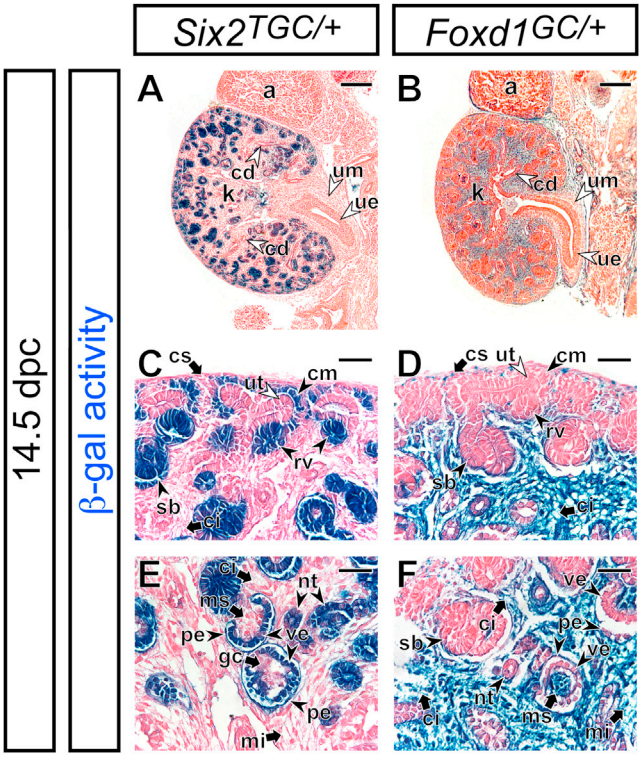

Figure 1. The *Six2*+ Cap Mesenchyme and *Foxd1*+ Cortical Stroma Give Rise to Distinct Cellular Lineages of the Kidney

β-gal-stained (blue) kidneys from $Six2^{TGC/+}$; $R26R^{lacZ/+}$ (A, C, and E), and $Foxd1^{GC/+}$; $R26R^{lacZ/+}$ (B, D, and F) embryos at 14.5 dpc counterstained with eosin (pink).

(A and B) Whole kidney.

(C–F) Higher magnification of the nephrogenic zone (C and D) and renal cortex with glomeruli (E and F).

a, adrenal gland; cd, collecting duct; ci, renal cortical interstitium; cm, cap mesenchyme; cs, cortical stroma; k, kidney; mi, renal medullary interstitium; ms, mesangium; nt, nephron tubule; pe, parietal epithelium; rv, renal vesicle; sb, S-shaped body; ue, ureter epithelium; um, ureter mesenchyme; ut, ureteric tip; ve, visceral epithelium (podocyte). Scale bars, 200 μm (A and B) and 50 μm (C–F).

suggests a more complicated relationship among these stromal and nephron progenitor populations. There are three possible explanations for this result. First, *Foxd1* may be activated transiently in a variable pattern within multiple regions of a subset of maturing nephrons. A molecular heterogeneity of this kind seems unlikely given our knowledge of nephron patterning and function. Furthermore, even if *Foxd1* is transiently expressed in differentiating nephron epithelia, it is expected that such transient expression will result in a low level of Cre protein insufficient for DNA recombination. Second, there is a continual low-level contribution of *Foxd1*+ cortical stromal cells to repopulate the *Six2*+ nephron progenitors as kidney development proceeds. However, pulse labeling of *Foxd1*+ cortical stromal cells in $Foxd1^{GCE/+}$; $R26R^{lacZ/+}$ kidneys by tamoxifen injections at 11.5, 12.5, or 14.5 dpc did not result in β-gal+ cells in the nephron epithelium perinatally (Figures S4B, S4D, and S4F; data not shown), indicating that there is no contribution of *Foxd1*+ cells to the nephron epithelial cells at these stages after the onset of kidney development.

Finally, in the initial separation of *Foxd1*+ and *Six2*+ lineages at the onset of kidney development, some plasticity may remain within *Foxd1*+ cells such that they can secondarily convert to the *Six2*+ lineage. Although we did not detect *Foxd1-GFPCre* transgene expression in the SIX2+ cap mesenchyme at 11.5, 12.5, and 15.5 dpc, β-gal+ descendant cells from the *Foxd1*+ population were observed in the SIX2+ cap mesenchyme of $Foxd1^{GC/+}$; $R26R^{lacZ/+}$ kidneys by 11.5 dpc (Figure S5). β-gal+ SIX2+ cells were more frequently observed in the outer half of the SIX2+ population close to the cortical stroma (65.9% at 11.5 dpc [n = 41] and 57.1% at 12.5 dpc [n = 21]). Subsequently, although we never observed overlap of *Foxd1*-driven GFP expression and SIX2, the fraction of β-gal+ cells within the SIX2+ population increased significantly as nephrons differentiate between 12.5 and 15.5 dpc (1.53% ± 0.48% to 3.31% ± 0.16%, n = 3; $p < 0.05$, unpaired t test) (Figure S4I).

Together, our results indicate that there is a low transient reassignment within a *Foxd1*+ cell type to *Six2*+*Foxd1*− nephron progenitors but likely only at the onset of kidney development. By 11.5 dpc, all *Six2*+ and *Foxd1*+ mesenchymal cells are restricted to mutually exclusive nephron and stromal lineages, respectively. The marginal contribution of *Foxd1*+ descendants to the *Six2*+ population results in a sporadic contribution to the nephrons of the mature kidney: most nephrons are unlabeled by mesenchymal *Foxd1*+ descendants. Those that show a variable contribution likely reflect the proportion of these descendants in the nephron precursor, the renal vesicle. Our data cannot exclude the possibility of transient SIX2+ FOXD1+ cells at different time points that our methods cannot detect.

The *Foxd1*+ Cortical Stroma Is a Stromal Progenitor Population

We further determined cell types derived from *Foxd1*+ cortical stromal cells at a molecular level. We examined *Foxd1*+ cortical stroma-derived β-gal+ cells in $Foxd1^{GC/+}$; $R26R^{lacZ/+}$ kidneys at 15.5 dpc using the following cell-type-specific markers: cytokeratin (KRT) (ureteric tip and collecting duct); LIV2 (capsule and the outermost connective tissue); Wilms tumor 1 (WT1) (cap mesenchyme, visceral epithelium/podocytes); platelet-derived growth factor (PDGF) receptor β (PDGFRB; interstitium, glomerular mesangium, and pericytes); FLK1 (endothelium); CDKN1C (P57KIP2; a subset of the medullary interstitium); F4/80

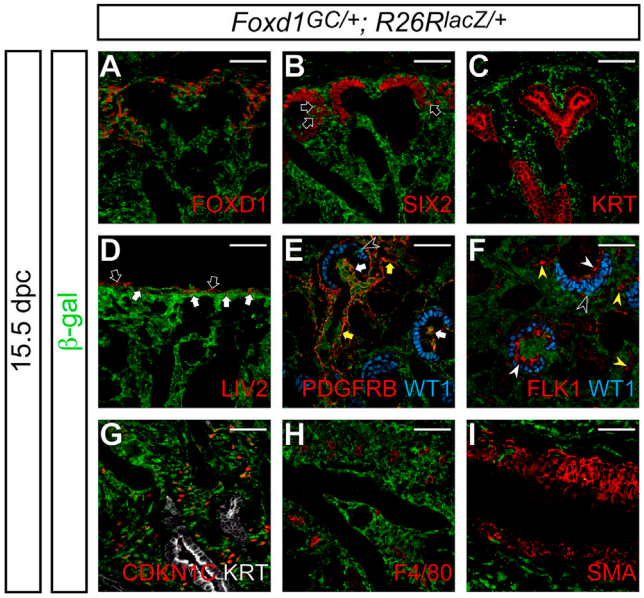

Figure 2. The *Foxd1*+ Cortical Stroma Is a Progenitor Population for Stromal Tissues in the Kidney

Confocal immunofluorescence images of *Foxd1*$^{GC/+}$; *R26R*$^{lacZ/+}$ kidneys at 15.5 dpc with anti-β-gal staining (green).

(A–D) Nephrogenic zone.

(A) FOXD1 (red).

(B) SIX2 (red). Black arrows indicate β-gal+ SIX2+ cap mesenchyme cells.

(C) KRT (red).

(D) LIV2 (red). White and black arrows indicate inner LIV2+ β-gal+ cells in the renal capsule and outer LIV2+ β-gal− cells in the connective tissue, respectively.

(E and F) Renal cortex with glomeruli.

(E) PDGFRB (red) and WT1 (blue). Yellow and white arrows indicate PDGFRB+ β-gal+ pericytes and mesangial cells, respectively.

(F) FLK1 (red) and WT1 (blue). Yellow and white arrowheads indicate FLK1+ β-gal− vascular cells in the renal cortex outside of the glomerulus and within the glomerular tuft, respectively. Black arrowheads in (E) and (F) indicate WT1+ β-gal+ podocytes.

(G and H) Renal medulla.

(G) CDKN1C (P57KIP2, red) and KRT (white).

(H) F4/80 (red).

(I) Ureter with SMA (red).

Scale bars, 50 μm.

(EMR1; macrophages); and smooth muscle actin α (aSMA/ACTA2; smooth muscle) (Figure 3).

In the nephrogenic zone, all FOXD1+ cortical stromal cells were β-gal+, no overlap of β-gal+ cells was observed in KRT+ ureteric tip/stalk cells, and only rare β-gal+ cells were noted among the SIX2+ cap mesenchyme, as described above (Figures 2A–2C). LIV2 staining was observed in the two outermost tissue layers of the kidney: the surface connective tissue, and an underlying layer of the capsule (Levinson et al., 2005) (data not shown). Although β-gal+ cells were detected in the inner LIV2+ renal capsule, a subpopulation of the FOXD1+ cortical stroma, no β-gal+ cells were observed in the outermost LIV2+ connective tissue (Figure 2D). In the renal cortex, PDGFRB+ cells, including cortical interstitial cells, mesangial cells of the glomerulus, and pericytes outside of the glomerulus, were β-gal+, but FLK1+ endothelial cells were β-gal− (Figures 2E and 2F; data not shown). As expected, some *Foxd1*+ maturing podocytes were labeled such that all podocytes were β-gal+ in the adult kidney (black arrowheads in Figures 2E, 2F, and S4C; data not shown). In the renal medulla, a subset of medullary interstitial cells expressing CDKN1C+ (P57KIP2+) (Yu et al., 2009; Zhang et al., 1997) was β-gal+ (Figure 2G), but F4/80+ macrophages were β-gal− (Figure 2H). Although SMA+ cells in the kidney were derived from *Foxd1*+ cells, β-gal+ cells were not observed in the SMA+ smooth muscle of the ureter (Figure 2I). Importantly, we observed no evidence of direct *Foxd1* expression in cortical/medullary interstitial cells, mesangial cells, or pericytes. Taken together, these data suggest that *Foxd1*+ cortical stromal cells contribute to stromal cells of the kidney including cortical and medullary interstitial cells, mesangial cells, and pericytes but that smooth muscle cells in the ureter have an independent origin (Bohnenpoll et al., 2013; Boyle et al., 2014; Humphreys et al., 2008, 2010; Lin et al., 2014; Wang et al., 2009).

Tempo-Spatial Patterns for Stroma Formation from the *Foxd1*+ Cortical Stroma during Kidney Development

To examine whether there is an ongoing commitment of *Foxd1*+ cortical stromal cells to stromal lineages, we used the tamoxifen-dependent *Foxd1-GCE* allele to label *Foxd1*+ cortical stromal cells at later stages of kidney development. We confirmed that the recombinase activity of the eGFPCreER^{T2} triple-fusion protein was completely tamoxifen dependent: no background recombination was detected without tamoxifen administration in the developing kidney (Figures 3A, 3E, 3I, 3M, and 3Q), as we previously observed with a *Six2-eGFPCreER*^{T2} allele (Kobayashi et al., 2008).

The *Foxd1*+ cortical stromal cells of *Foxd1*$^{GCE/+}$; *R26R*$^{lacZ/+}$ embryos were labeled by tamoxifen induction at 10.5, 12.5, or 14.5 dpc. β-gal activity was observed at 19.5 dpc in stromal cells of the kidney in embryos from dams injected with tamoxifen at all time points (Figures 3B–3D and 3F–3H). However, whereas tamoxifen injection at 10.5 dpc resulted in β-gal+ stromal cells along the entire radial axis of the kidney from the cortex to inner medulla (papilla) (Figures 3J, 3N, and 3R), 12.5 dpc injections did not label cells in the tip of the inner medulla (Figures 3K, 3O, and 3S), and 14.5 dpc injections showed β-gal+ stromal cells limited to

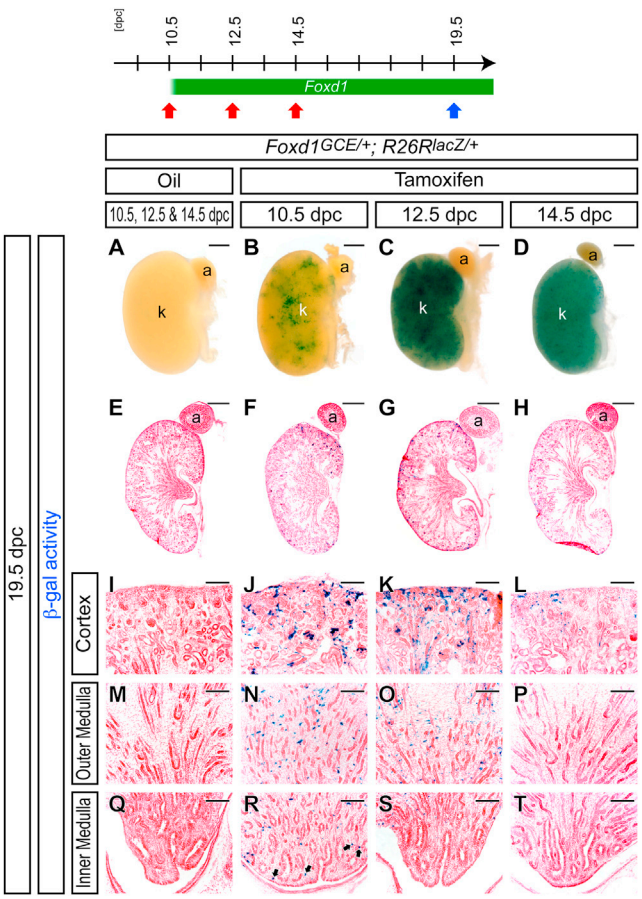

Figure 3. The *Foxd1*+ Cortical Stroma Contributes to Stromal Tissues throughout Kidney Organogenesis

β-gal-stained (blue) kidneys from *Foxd1*$^{GCE/+}$; *R26R*$^{lacZ/+}$ embryos at 19.5 dpc after three successive injections of oil vehicle only at 10.5, 12.5, and 14.5 dpc (A, E, I, M, and Q) or after a single injection of 2 mg tamoxifen at 10.5 dpc (B, F, J, N, and R), 12.5 dpc (C, G, K, O, and S), or 14.5 dpc (D, H, L, P, and T).

(A–D) Whole-mount view.

(E–T) Sections counterstained with eosin (pink).

(E–H) Whole kidney.

(I–L) Nephrogenic zone and renal cortex.

(M–P) Outer renal medulla.

(Q–T) Inner renal medulla (papilla). Arrows in (R) indicate β-gal+ interstitial cells in the inner medulla adjacent to the pelvic urothelial lining.

a, adrenal gland; k, kidney. Scale bars, 500 μm (A–H) and 100 μm (I–T).

the cortical interstitium (Figures 3L, 3P, and 3T). These data indicate that *Foxd1*+ cortical stromal cells continuously contributed to stromal lineages throughout kidney development and that there was a temporal restriction where later differentiating cells arising from the *Foxd1*+ progenitor compartment were cortically restricted. Interestingly, the radial restriction of β-gal+ stromal cells was still evident in the adult kidney, suggesting that radial domains once established were relatively stable within stromal tissues of the mature kidney (Figure S6).

The pulse labeling of *Foxd1*$^{GCE/+}$; *R26R*$^{lacZ/+}$ at 10.5, 12.5, and 14.5 dpc prior to FOXD1 expression in podocytes of maturing glomeruli did not label podocytes (Figures 3 and 4; data not shown), suggesting that podocytes are not derived from the *Foxd1*+ cortical stroma. The β-gal expression in a subset of podocytes in *Foxd1*$^{GC/+}$; *R26R*$^{lacZ/+}$ embryonic kidneys is due to *Foxd1-eGFPCre* activity directly in *Foxd1*+ podocytes.

Coordinated Differentiation from Nephron and Stromal Progenitor Populations during Kidney Organogenesis

Nephron formation also demonstrates a temporal restriction along the radial axis of the kidney (Boyle et al., 2008), suggesting that nephron and stromal progenitor populations may differentiate in a coordinated manner during kidney organogenesis. To test this possibility, we examined the cellular contributions from the *Six2*+ cap mesenchyme and *Foxd1*+ cortical stroma at different stages of kidney organogenesis. Because the differentiating loop of Henle of newly formed nephrons extends into the previously generated medullary interstitium, we analyzed podocytes and mesangial cells derived from the cap mesenchyme and cortical stroma, respectively, within the glomerulus, where temporal differentiation of the nephron and stromal compartments is maintained.

Tamoxifen induction at 14.5 dpc in *Six2*$^{GCE/+}$; *R26R*$^{lacZ/+}$ embryos resulted in β-gal activity in the cap mesenchyme and main body of the nephron in the renal cortex at 19.5 dpc, including nephrin+ (NPHS1+) podocytes of the less-differentiated capillary loop-stage glomerulus localized to the outer cortex (Figures 4B, 4F, 4J, and 4R). However, β-gal+ cells were not observed in the more differentiated glomeruli that formed at earlier developmental stages and are positioned deeper within the cortical region (Figures 4F, 4N, and 4V). A similar labeling and analysis of the *Foxd1*+ cortical stroma in *Foxd1*$^{GCE/+}$; *R26R*$^{lacZ/+}$ kidneys resulted in β-gal activity in stromal tissues of the renal cortex, the PDGFRB+ mesangium of the capillary loop-stage glomerulus (Figures 4C, 4G, 4K, and 4S), but not maturing-stage glomeruli (Figures 4G, 4O, and 4W). To compare contributions from the *Six2*+ cap mesenchyme and *Foxd1*+ cortical stroma directly, both progenitor populations were labeled in *Six2*$^{GCE/+}$; *Foxd1*$^{GCE/+}$; *R26R*$^{lacZ/+}$ kidneys at 14.5 dpc. β-gal activity was observed in both nephrin+ (NPHS1+) podocytes and PDGFRB+ mesangial cells of the capillary loop-stage glomerulus, but not the maturing-stage glomerulus (Figures 4D, 4H, 4L, 4P, 4T, and 4X). As expected, no β-gal activity was

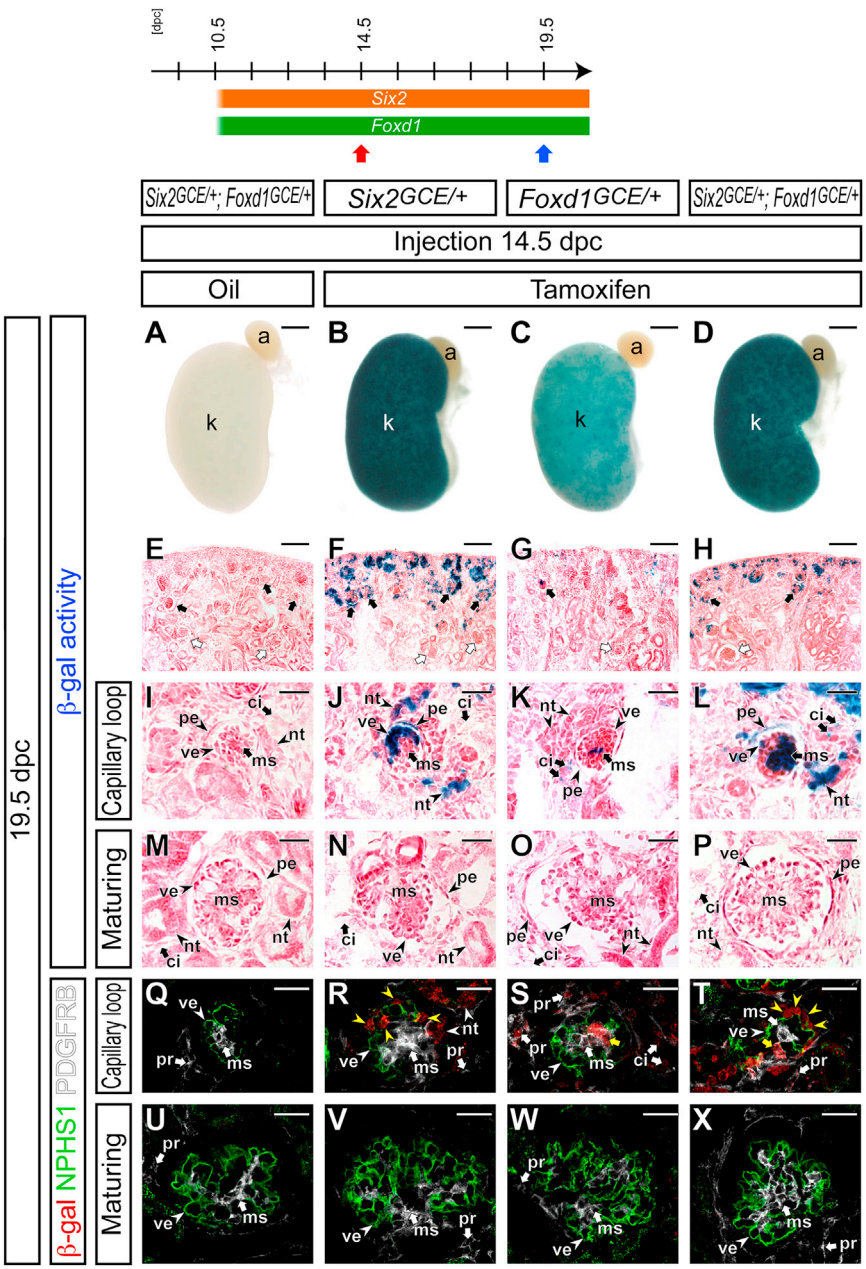

Figure 4. *Six2*+ Cap Mesenchymal Cells and *Foxd1*+ Cortical Stromal Cells Differentiate in a Coordinated Manner

Kidneys at 19.5 dpc from *Six2*$^{GCE/+}$; *Foxd1*$^{GCE/+}$; *R26R*$^{lacZ/+}$ mice with oil-only injection at 14.5 dpc (A, E, I, M, Q, and U), *Six2*$^{GCE/+}$; *R26R*$^{lacZ/+}$ with 6 mg tamoxifen at 14.5 dpc (B, F, J, N, R, and V), *Foxd1*$^{GCE/+}$; *R26R*$^{lacZ/+}$ with 6 mg tamoxifen at 14.5 dpc (C, G, K, O, S, and W), and *Six2*$^{GCE/+}$; *Foxd1*$^{GCE/+}$; *R26R*$^{lacZ/+}$ with 6 mg tamoxifen at 14.5 dpc (D, H, L, P, T, and X).

(A–D) β-gal-stained (blue) whole-mount kidney.

(E–P) β-gal-stained (blue) sections counterstained with eosin (pink).

(E–H) Nephrogenic zone and renal cortex. Black arrows and white arrows indicate capillary loop-stage and maturing-stage glomeruli, respectively.

(I–L) Capillary loop-stage glomerulus.

(M–P) Maturing-stage glomerulus.

(Q–X) Confocal immunofluorescence images with anti-β-gal (red), a podocyte marker anti-NPHS1 (nephrin, green), and a mesangium marker anti-PDGFRB (white).

(Q–T) Capillary loop-stage glomerulus. Yellow arrowheads and yellow arrows in (R)–(T) indicate the β-gal+ NPHS1+ podocytes and β-gal+ PDGFRB+ mesangial cells, respectively.

(U–X) Maturing-stage glomerulus.

a, adrenal gland; ci, renal cortical interstitium; k, kidney; ms, mesangium; nt, nephron tubule; pe, parietal epithelium; pr, pericyte; ve, visceral epithelium (podocyte). Scale bars, 500 μm (A–D), 100 μm (E–H), and 25 μm (I–X).

detected in oil-injected, carrier controls (Figures 4A, 4E, 4I, 4M, 4Q, and 4U). These data suggest that differentiation of stromal cells from the *Foxd1*+ progenitor population temporally and spatially coordinates with differentiation of the adjacent *Six2*+ progenitor pool into nephrons.

Foxd1+ Cortical Stromal Cells Are Maintained by Self-Renewal

To analyze the stromal progenitor population quantitatively, we performed fluorescence-activated cell sorting (FACS) analysis of *Foxd1-GFP*+ cells in *Foxd1*$^{GCE/+}$ kidneys to determine the cell number of *Foxd1*+ cells during early-to-mid stages of nephrogenesis. We observed that *Foxd1*+ cells in a single kidney undergo a 22.5-fold increase from 4,485 ± 1,081 cells at 11.5 dpc (n = 12) to 101,068 ± 13,004 cells at 14.5 dpc (n = 6). Podocyte labeling is insignificant at this time (Figures 1B and 1F); thus, the majority of *Foxd1*+ cells at 14.5 dpc are within the cortical stroma that harbors *Six2*+ nephron progenitors and *Ret*+ ureteric epithelial progenitors (Shakya et al., 2005). Given a continual contribution of *Foxd1*+ progenitor cells to differentiated

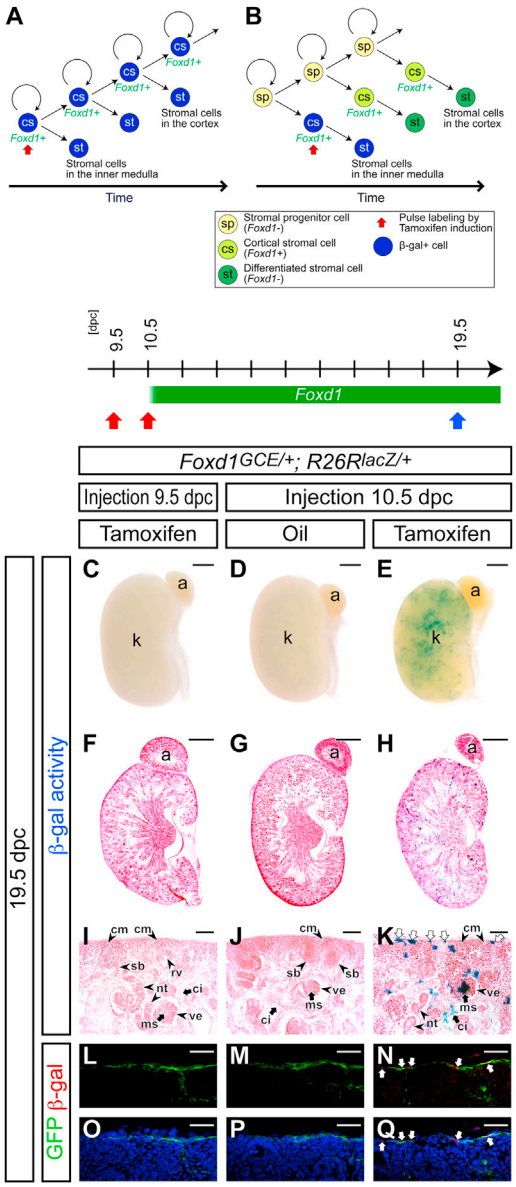

Figure 5. *Foxd1*+ Cortical Stromal Cells Self-Renew

(A and B) Models for maintenance of cortical stromal cells.

(A) A pulse-labeled β-gal+ (blue) *Foxd1*+ cortical stromal (cs) cell produces another β-gal+ *Foxd1*+ cortical stromal cell, which results in retention of β-gal+ cells in the *Foxd1*+ cortical stroma. Differentiated stromal cells (st) are β-gal+ cells along the cortico-medullary axis throughout kidney organogenesis.

(B) A *Foxd1*− stromal precursor population (sp) that generates *Foxd1*+ cortical stromal cells (cs) resides outside of the *Foxd1*+ population. Contribution of β-gal− cells from the *Foxd1*− stromal precursor population (sp) dilutes the pulse-labeled β-gal+ (blue) cells in the *Foxd1*+ cortical stroma (cs; light green). Only differentiated stromal cells (st) at early stages will be β-gal+ (blue) cells that will be seen in the inner medulla (papilla), but stromal cells in the renal cortex (st; dark green), which differentiate at later stages, will be β-gal−.

stromal derivatives, these data indicate an extensive expansion of the *Foxd1*+ stromal progenitor pool during kidney organogenesis.

To examine whether expansion of the *Foxd1*+ cell compartment occurs by self-renewal (Figure 5A) or through repopulation from external *Foxd1*− progenitor cells (Figure 5B), we performed a developmental pulse-chase experiment labeling *Foxd1*+ cells at the onset of kidney development (10.5 dpc) and examined retention of β-gal-labeled cells in the *Foxd1*+ stromal progenitors at birth (19.5 dpc). To determine the dynamics of Cre recombination activity, we injected 2 mg of tamoxifen into dams at 9.5 dpc, 1 day before the onset of *Foxd1* expression in the metanephric region (Bohnenpoll et al., 2013; Mugford et al., 2008). No β-gal+ cells were observed in the 19.5 dpc kidney (Figures 5C, 5F, 5I, 5L, and 5O), consistent with a time window of tamoxifen activity of less than 24 hr for this dose as we reported previously (Kobayashi et al., 2008). When tamoxifen was injected at 10.5 dpc, we observed a significant contribution of β-gal+ cells within the *Foxd1-GFP*+ cortical stroma at 19.5 dpc (Figures 5E, 5H, 5K, 5N, and 5Q). Between 10% and 20% cells of *Foxd1-GFP*+ cortical stromal cells were β-gal+ at 19.5 dpc with some variation between dams and even between littermates (Figures 5N and 5Q; data not shown). No β-gal+ cells were detected in any oil-injected controls (Figures 5D, 5G, 5J, 5M, and 5P), indicating that these data are absolutely tamoxifen dependent. Considering our observations that even over a brief period from 11.5 to 14.5 dpc, the number of *Foxd1*+ cells increases 22.5-fold and that stromal cells are continuously differentiating from the *Foxd1*+ progenitor population, collectively, the results are most consistent with self-renewal within the *Foxd1*+ cortical stroma as the main driver for the maintenance and expansion of the stromal progenitor pool. Although we cannot exclude the minor contribution of *Foxd1*− cells

(C–Q) *Foxd1*$^{GCE/+}$; *R26R*$^{lacZ/+}$ kidneys at 19.5 dpc after injection of 2 mg tamoxifen at 9.5 dpc (C, F, I, L, and O) and 10.5 dpc (E, H, K, N, and Q), and oil only at 10.5 dpc (D, G, J, M, and P).

(C–E) Whole-mount β-gal-stained (blue) kidneys.

(F–H) Sections of β-gal-stained (blue) kidneys counterstained with eosin (pink).

(I–K) Higher magnification of the cortical region in (F)–(H), respectively. White arrows in (K) indicate multiple β-gal+ cells in the cortical stroma.

(L–Q) Confocal immunofluorescence images with anti-GFP (green), anti-β-gal (red), with (L–N) or without (O–Q) Hoechst (blue) staining. White arrows in (N) and (Q) indicate β-gal+ GFP+ cortical stromal cells.

a, adrenal gland; ci, renal cortical interstitium; cm, cap mesenchyme; k, kidney; ms, mesangium; nt, nephron tubule; pe, parietal epithelium; pr, pericyte; rv, renal vesicle; ve, visceral epithelium (podocyte). Scale bars, 500 μm (C–H) and 50 μm (I–Q).

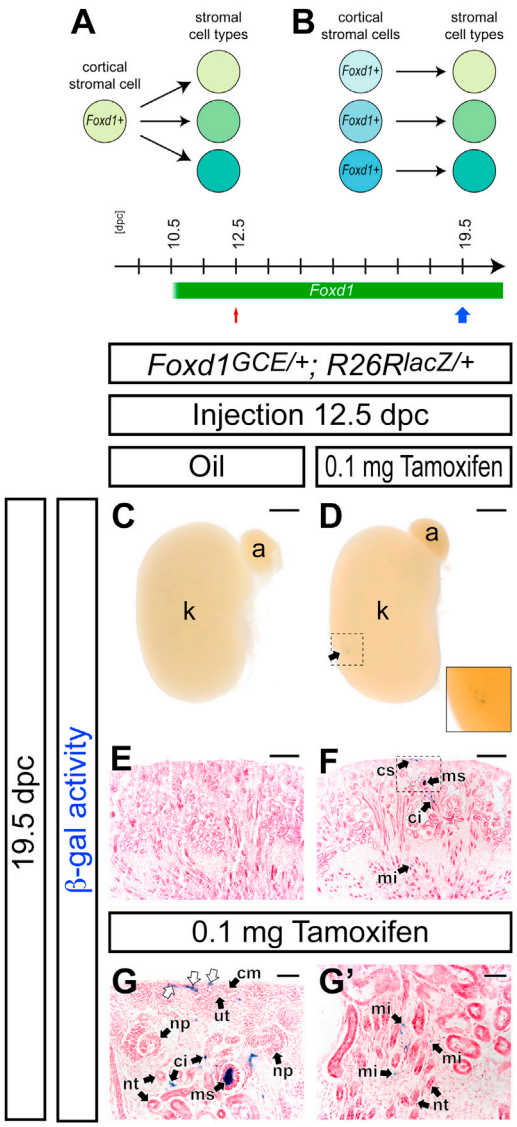

Figure 6. *Foxd1*+ Cortical Stromal Cells Can Be Multipotent Stromal Progenitors

(A and B) Models for developmental potential of *Foxd1*+ cells.

(A) A *Foxd1*+ cortical stromal cell retains multipotency to differentiate into different stromal tissues.

(B) Developmental potential of a *Foxd1*+ cell is restricted to limited stromal cell types within the *Foxd1*+ cortical stroma.

(C–G′) β-gal-stained (blue) kidneys from *Foxd1*$^{GCE/+}$; *R26R*$^{lacZ/+}$ embryos at 19.5 dpc after injection of oil only (C and E), and 0.1 mg tamoxifen (D, F, G, and G′) at 12.5 dpc.

(C and D) Whole-mount view. The inset in (D) shows a higher magnification of a clone in the dashed region. The arrow in (D) indicates a β-gal+ clone.

(E and F) Sections counterstained with eosin (pink).

(G and G′) Adjacent sections 96 μm apart showing the same clone. (G) is a higher magnification of the dashed region in (F). White arrows in (G) indicate multiple β-gal+ cells in the cortical stroma.

to the cortical stroma, we did not observe a reduced contribution of labeled cells along the medullary and cortical interstitium (Figure 5H; data not shown), suggesting that any contribution from *Foxd1*− cells is not likely to constitute a substantive mechanism maintaining cortical stromal populations.

A *Foxd1*+ Cell Can Give Rise to Multiple Stromal Cell Types

To determine whether multiple interstitial cell types can arise from clonal labeling of a *Foxd1*+ stromal progenitor cell (Figures 6A and 6B), we optimized dosages of tamoxifen for clonal analysis (Kobayashi et al., 2008). With injection of 0.1 mg tamoxifen at 12.5 dpc, we observed well-separated rare, tamoxifen-dependent β-gal+ clusters in the kidney at 19.5 dpc (1.95 ± 1.00 clusters per kidney; n = 20) (Figures 6C–6F), indicating that these rare clusters are likely derived from a single *Foxd1*+ cortical stromal cell. We analyzed 13 such clusters in kidneys with 3 clonal clusters or less at 19.5 dpc. Within a cluster, β-gal+ cells were observed within a limited area along the cortico-medullary axis (Figures 6D and 6F), indicating that renal stromal cells do not actively change relative positions not only along the radial axis (Figure 3) but also along the planes perpendicular to the cortico-medullary axis of the developing kidney. Multiple cells exhibiting β-gal activity were observed in the zone of *Foxd1*+ stromal progenitor cells, consistent with our earlier data on self-renewal of this population (white arrows in Figure 6G). In differentiated stromal tissues, β-gal activity was observed in the cortical interstitium, mesangium, and medullary interstitium within a single cluster (Figures 6F, 6G, and 6G′). Thus, *Foxd1*+ cortical stromal cells likely contain a multipotent cell type capable of generating regionally diverse stromal cell types.

Foxd1 Function Is Dispensable for Regulation of the Stromal Lineage

The transcription factor *Foxd1* plays important roles in kidney development. In the absence of *Foxd1* function, the renal capsule formed abnormally, and the cap mesenchyme is thickened with retarded nephron differentiation (Fetting et al., 2014; Hatini et al., 1996; Levinson et al., 2005). Because *Foxd1* is expressed in the stromal progenitor population, it is possible that *Foxd1* regulates the stromal lineage during kidney development. To address this question, we examined the fate map of *Foxd1*+ cortical stromal cells in the absence of *Foxd1* activity.

a, adrenal gland; ci, renal cortical interstitium; cm, cap mesenchyme; cs, cortical stroma; k, kidney; mi, renal medullary interstitium; ms, mesangium; np, nephron precursor; nt, nephron tubule; ut, ureteric tip. Scale bars, 500 μm (C and D), 200 μm (E and F), and 50 μm in (G and G′).

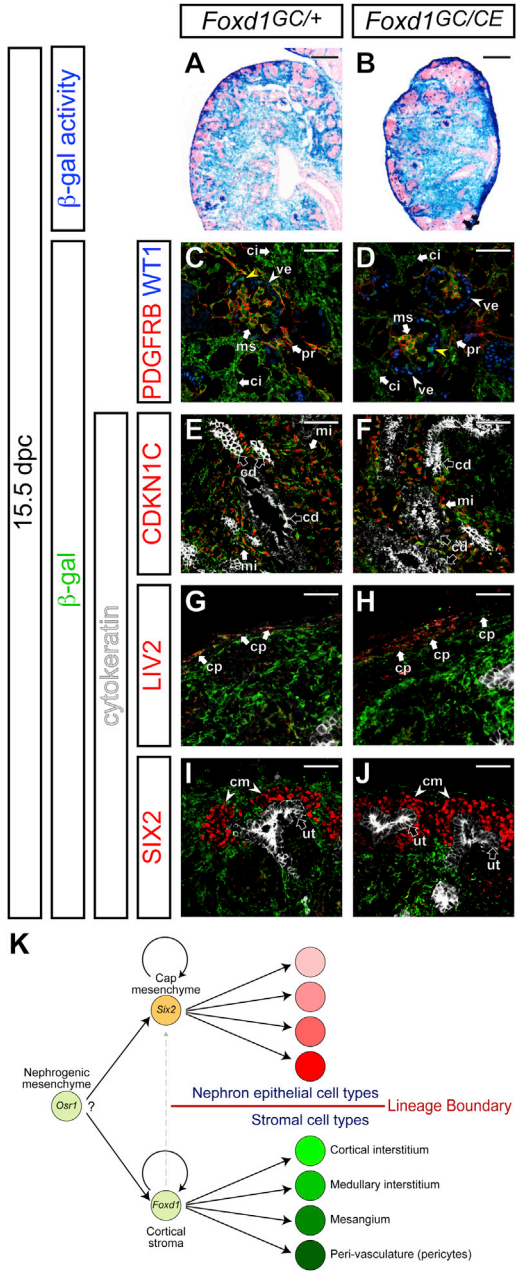

Figure 7. *Foxd1* Activity Is Dispensable for Cell-type Specification of Stromal Tissues

Kidneys from *Foxd1*$^{GC/+}$; *R26R*$^{lacZ/+}$ (A, C, E, G, and I) and *Foxd1*$^{GC/CE}$; *R26R*$^{lacZ/+}$ (B, D, F, H, and J) embryos at 15.5 dpc.

(A and B) β-gal-stained (blue) sections counterstained with eosin (pink).

(C–J) Confocal immunofluorescence imaging with anti-β-gal (green) and anti-KRT (white) staining in (E)-(J). KRT is expressed in the ureteric tip and collecting duct.

(C and D) PDFGRB (red) and WT1 (blue). Yellow arrowheads indicate β-gal+ WT1+ podocytes.

(E and F) P57KIP2 (CDKN1C, red).

(G and H) LIV2 (red).

(I and J) SIX2 (red).

cd, collecting duct; ci, renal cortical interstitium; cm, cap mesenchyme; cp, capsule; mi, renal medullary interstitium; ms, mesangium; pr, pericyte; ut, ureteric tip; ve, visceral epithelium (podocyte).

(K) A model for cellular differentiation from mesenchymal progenitor populations during mammalian kidney development. The *Six2*+ cap mesenchyme and *Foxd1*+ cortical stroma are a multipotent self-renewing progenitor population for nephron epithelial and renal stromal cell types. Although *Six2*+ cells differentiate into all cell types of the main body of the nephron, *Foxd1*+ cortical stromal cells contribute to all stromal cells in the kidney, including cortical and medullary interstitial cells, mesangial cells, and pericytes. Only around the onset of kidney development, a small fraction of *Foxd1*+ cells becomes *Six2*+ cells (gray dashed arrow). Thereafter, the *Six2*+ cell-derived nephron lineage and *Foxd1*+ cell-derived stromal lineage form compartments with a lineage boundary throughout kidney development. Although the *Osr1*+ nephrogenic mesenchyme can contribute to both *Six2*+ cap mesenchyme and *Foxd1*+ cortical stroma, currently, it is unclear whether a single *Osr1*+ cell can differentiate into both *Six2*+ and *Foxd1*+ mesenchymal progenitor cells.

Scale bars, 200 μm (A and B) and 50 μm (C–J).

Foxd1$^{GC/CE}$ mice displayed a similar phenotype to that previously described for *Foxd1* null mutant mice: the horseshoe kidneys containing the accumulated cap mesenchyme ectopically along the cortico-medullary axis, and the thickened capsule on the cortical surface (Hatini et al., 1996; Levinson et al., 2005). Thus, the creation of the targeted allele appears to phenocopy the existing *Foxd1* null mutants. When *Foxd1*$^{GC/CE}$; *R26R*$^{lacZ/+}$ kidneys were examined, we observed β-gal activity in a similar range of cell types within the 15.5 dpc kidneys to *Foxd1*$^{GC/+}$; *R26R*$^{lacZ/+}$controls with a single active *Foxd1* allele (Figures 7A and 7B). In the renal cortex, β-gal+ cells were detected in PDGFRB+ mesangial cells and pericytes (Figures 7C and 7D). No evidence was found for the additional contribution of β-gal+ cells to the *Six2*+ nephron progenitor pool or to cells of the nephron, except for the expected contribution to late-stage WT1+ podocytes (Figures 7C, 7D, 7I, and 7J). β-gal+ cells were observed in the CDKN1C+ (P57KIP2+) renal medullary interstitium, the LIV2+ renal capsule, but not in the KRT+ collecting duct (Figures 7E–7J). Thus, *Foxd1* activity is dispensable for specification and differentiation of the stromal interstitial lineage within the mouse kidney.

DISCUSSION

The *Foxd1*+ Cortical Stroma Demarcates the Stromal Progenitor Population during Kidney Organogenesis

Our data indicate that *Foxd1*+ cortical stromal cells contribute to renal cortical and medullary interstitial cells,

mesangial cells, and pericytes of the mammalian kidney (Figure 7K). The origin of the kidney stromal cells is somewhat controversial. In the mouse, analysis of *Osr1*+ intermediate and dorsal lateral plate mesoderm derivatives at 7.5–10.5 dpc showed that this population contributes to *Foxd1*+ stromal progenitors and *Six2*+ nephron progenitors. Thereafter, *Osr1* expression becomes restricted to the *Six2*+ cells as the lineage boundary is established between *Six2*+ and *Foxd1*+ progenitor compartments (Mugford et al., 2008). In the chick, labeling studies have suggested a paraxial mesoderm origin for *Foxd1*+ stromal progenitors (Guillaume et al., 2009). If *Foxd1* demarcates stromal progenitors in both systems, these data may suggest species difference or alternate mechanisms for distinct subsets of *Foxd1*+ cells.

Our analysis does not address whether the *Foxd1*+ cortical stroma is a homogeneous population where all *Foxd1*+ cells are stromal progenitor cells. Alternatively, the *Foxd1*+ cortical stroma may be a heterogeneous population where only a subset of *Foxd1*+ cells maintains a stromal-repopulating and broad differentiation capability. Indeed, the *Foxd1*+ cortical stroma consists of a cortical LIV2+ capsule and a medullary LIV2− nephrogenic interstitium. The current study does not distinguish whether stromal progenitor cells exist in the capsule, nephrogenic interstitium, or both. Moreover, it is possible that each domain contains heterogeneous cells with different properties. Additional fate mapping for subdomains within the *Foxd1*+ cortical stroma will be required to address these possibilities.

Distinct Multipotent Self-Renewing Progenitor Populations Direct Mammalian Kidney Organogenesis

Our data reinforce the critical cellular makeup and distinct developmental properties of the niche present at each branch tip of the developing ureteric tree in the mammalian kidney. Within the ureteric epithelium are the mitotically active *Ret*+ progenitors whose renewal establishes new branch tips in the arborizing collecting duct system and whose commitment generates the maturing medullary and cortical stalks of the differentiating ureteric epithelial network (Shakya et al., 2005). Immediately adjacent to the ureteric branch tips lie the *Six2*+ cap mesenchyme, a multipotent self-renewing progenitor population for the main body of the nephron. Our data demonstrate that the *Foxd1*+ population that surrounds the *Six2*+ domain is a distinct multipotent self-renewing progenitor population for renal stromal cells.

Six2 and *Foxd1* expression correlates with distinct mesenchymal progenitor populations. Both genes are rapidly downregulated on commitment and movement of cells from the ureteric tip zone suggesting that expression of these markers, and maintenance of progenitor properties, is dependent on this cortical niche. Our observation of the lineage boundary between the *Six2*+ cap mesenchyme-derived nephron epithelial compartment and *Foxd1*+ cortical stroma-derived stromal compartment suggests that these cell types are largely independent progenitor pools from the onset of kidney organogenesis at 10.5 dpc, consistent with our previous observation from a clonal analysis of *Osr1*+ metanephric mesenchyme cells at 9.5 dpc (Mugford et al., 2008). However, our cell fate analysis indicates that a fraction of cells transiently activates *Foxd1* in a cell that becomes a *Six2*+ nephron progenitor. Thus, *Foxd1* activity does not appear to result in an irreversible commitment to a stromal progenitor fate, consistent with our analysis of *Foxd1* null kidneys. The factor(s) responsible for establishing these lineage boundaries is unclear, but a number of transcriptional regulators have been mapped to each of these cellular compartments in the developing kidney (Brunskill et al., 2008; Mugford et al., 2009).

Throughout kidney organogenesis, the *Six2*+ and *Foxd1*+ cells are retained in the cortical niche. As the developing kidney grows outward, these progenitor populations leave behind differentiated derivatives, and the kidney grows along a radial medullary to cortical axis with less mature nephron and stromal cells in more cortical regions at all developmental stages. The cellular localization of progenitor compartments and their progressive commitment could facilitate the coordination of differentiation of the distinct nephron and stromal lineages during kidney organogenesis. Consistent with this view, pulse labeling shows corecruitment of cell types derived from *Six2*+ and *Foxd1*+ cells into distinct components of assembling glomeruli.

Recently, it was proposed that the outer and inner regions within the cap mesenchyme may have different properties (Das et al., 2013). *Foxd1*+ descendant *Six2*+ cells tend to localize in the outer half of the SIX2+ cap mesenchyme just after the onset of kidney development. Although this bias along the outer-inner axis in the cap mesenchyme decreases gradually, the fraction of *Foxd1*+ descendant cells among the entire *Six2*+ population increases during kidney development, though there is no evidence of additional *Foxd1*+ cell recruitment into the *Six2*+ pool during these stages. These data indicate that *Foxd1*+ descendant *Six2*+ cells in the outer region closer to the capsule may differentiate into the nephron less frequently than *Six2*+ cells lying closer to the ureteric epithelium, contrary to the recently proposed model where the outer cap mesenchymal cells differentiate, whereas the inner cap mesenchymal cells self-renew (Das et al., 2013). Alternatively, these *Foxd1*+ descendant *Six2*+ cells may have different properties from other *Six2*+ cells in the outer cap mesenchyme in cell proliferation/death and/or migration.

The relationship between developmental progenitor compartments within the kidney and the precise origins of some mature cell types that include the vasculature, macrophage, smooth muscle, and neural-associated components remain less clear, although our previous data suggest that vascular cells in the kidney and smooth muscle cells around the ureter are derived from parts of the *Osr1*+ intermediate mesoderm and lateral plate mesoderm at 8.5 dpc (Mugford et al., 2008). Our data also shed light on differences between the kidney and ureter. The ureter mesenchyme does not originate from the cap mesenchyme, cortical stroma, or ureteric bud. Consistent with this, the *Foxd1*− *Tbx18*+ mesenchyme between the kidney and nephric duct at the onset of kidney development contributes to the ureter mesenchyme (Bohnenpoll et al., 2013; Wang et al., 2009). Other evidence suggests a tail bud origin for these cells in the chick (Brenner-Anantharam et al., 2007), whereas the contribution of *Osr1*+ cell derivatives from 8.5 to 10.5 dpc to this population in the mouse points to a possible dorsal lateral plate origin (Mugford et al., 2008). Fate mapping analysis using additional tissue-specific transgenes will define progenitor populations for these cell types in the future.

EXPERIMENTAL PROCEDURES

Mouse Strains

Mice were generated and maintained as described in the Supplemental Experimental Procedures. All animal work was performed under the oversight by an institutional review board at the Harvard Center for Comparative Medicine.

FACS Analysis

FACS analysis of kidney cells was performed as described in the Supplemental Experimental Procedures.

Histology

Histology on kidneys was performed as described in the Supplemental Experimental Procedures.

X-Gal Staining

X-gal staining was performed as described previously (Kobayashi et al., 2004, 2005). Details are described in the Supplemental Experimental Procedures.

Immunofluorescence

Confocal immunofluorescence was performed as described previously (Kobayashi et al., 2008, 2011). Details are described in the Supplemental Experimental Procedures.

SUPPLEMENTAL INFORMATION

Supplemental Information includes Supplemental Experimental Procedures and six figures and can be found with this article online at http://dx.doi.org/10.1016/j.stemcr.2014.08.008.

ACKNOWLEDGMENTS

We thank Drs. Benjamin Humphreys, Joo-Seop Park, Stuart Shankland, Ed Laufer, and Cathy Mendelsohn for critical comments on the manuscript. We thank Dr. Kevin Eggan for v6.5 129/Sv × C57BL/6 F1 hybrid embryonic stem cells, Dr. Brian Sauer for *EGFP-Cre* construct, and Drs. Daniel Metzger and Pierre Chambon for *CreER*^{T2} construct. This study used data from the GenePaint database (http://www.genepaint.org) and GUDMAP database (http://www.gudmap.org). Work in A.K.'s laboratory was supported by a grant from the NIH (DK094933), Basil O'Connor Starter Scholar Research Award from the March of Dimes, Carl W. Gottschalk Research Scholar Grant from the American Society of Nephrology, and grants from the Harvard Stem Cell Institute. Work in A.P.M.'s laboratory was supported by a grant from the NIH (DK054364).

Received: December 11, 2013
Revised: August 11, 2014
Accepted: August 12, 2014
Published: September 18, 2014

REFERENCES

Bohnenpoll, T., Bettenhausen, E., Weiss, A.C., Foik, A.B., Trowe, M.O., Blank, P., Airik, R., and Kispert, A. (2013). Tbx18 expression demarcates multipotent precursor populations in the developing urogenital system but is exclusively required within the ureteric mesenchymal lineage to suppress a renal stromal fate. Dev. Biol. *380*, 25–36.

Boyle, S., Misfeldt, A., Chandler, K.J., Deal, K.K., Southard-Smith, E.M., Mortlock, D.P., Baldwin, H.S., and de Caestecker, M. (2008). Fate mapping using Cited1-CreERT2 mice demonstrates that the cap mesenchyme contains self-renewing progenitor cells and gives rise exclusively to nephronic epithelia. Dev. Biol. *313*, 234–245.

Boyle, S.C., Liu, Z., and Kopan, R. (2014). Notch signaling is required for the formation of mesangial cells from a stromal mesenchyme precursor during kidney development. Development *141*, 346–354.

Brenner-Anantharam, A., Cebrian, C., Guillaume, R., Hurtado, R., Sun, T.T., and Herzlinger, D. (2007). Tailbud-derived mesenchyme promotes urinary tract segmentation via BMP4 signaling. Development *134*, 1967–1975.

Brunskill, E.W., Aronow, B.J., Georgas, K., Rumballe, B., Valerius, M.T., Aronow, J., Kaimal, V., Jegga, A.G., Yu, J., Grimmond, S., et al. (2008). Atlas of gene expression in the developing kidney at microanatomic resolution. Dev. Cell *15*, 781–791.

Brunskill, E.W., Georgas, K., Rumballe, B., Little, M.H., and Potter, S.S. (2011). Defining the molecular character of the developing and adult kidney podocyte. PLoS ONE *6*, e24640.

Carroll, T.J., Park, J.S., Hayashi, S., Majumdar, A., and McMahon, A.P. (2005). Wnt9b plays a central role in the regulation of mesenchymal to epithelial transitions underlying organogenesis of the mammalian urogenital system. Dev. Cell *9*, 283–292.

Costantini, F. (2006). Renal branching morphogenesis: concepts, questions, and recent advances. Differentiation *74*, 402–421.

Costantini, F., and Kopan, R. (2010). Patterning a complex organ: branching morphogenesis and nephron segmentation in kidney development. Dev. Cell *18*, 698–712.

Das, A., Tanigawa, S., Karner, C.M., Xin, M., Lum, L., Chen, C., Olson, E.N., Perantoni, A.O., and Carroll, T.J. (2013). Stromal-epithelial crosstalk regulates kidney progenitor cell differentiation. Nat. Cell Biol. *15*, 1035–1044.

Dressler, G.R. (2009). Advances in early kidney specification, development and patterning. Development *136*, 3863–3874.

Fetting, J.L., Guay, J.A., Karolak, M.J., Iozzo, R.V., Adams, D.C., Maridas, D.E., Brown, A.C., and Oxburgh, L. (2014). FOXD1 promotes nephron progenitor differentiation by repressing decorin in the embryonic kidney. Development *141*, 17–27.

Guillaume, R., Bressan, M., and Herzlinger, D. (2009). Paraxial mesoderm contributes stromal cells to the developing kidney. Dev. Biol. *329*, 169–175.

Harding, S.D., Armit, C., Armstrong, J., Brennan, J., Cheng, Y., Haggarty, B., Houghton, D., Lloyd-MacGilp, S., Pi, X., Roochun, Y., et al. (2011). The GUDMAP database—an online resource for genitourinary research. Development *138*, 2845–2853.

Hatini, V., Huh, S.O., Herzlinger, D., Soares, V.C., and Lai, E. (1996). Essential role of stromal mesenchyme in kidney morphogenesis revealed by targeted disruption of Winged Helix transcription factor BF-2. Genes Dev. *10*, 1467–1478.

Herzlinger, D. (1995). Inductive interactions during kidney development. Semin. Nephrol. *15*, 255–262.

Humphreys, B.D., Valerius, M.T., Kobayashi, A., Mugford, J.W., Soeung, S., Duffield, J.S., McMahon, A.P., and Bonventre, J.V. (2008). Intrinsic epithelial cells repair the kidney after injury. Cell Stem Cell *2*, 284–291.

Humphreys, B.D., Lin, S.L., Kobayashi, A., Hudson, T.E., Nowlin, B.T., Bonventre, J.V., Valerius, M.T., McMahon, A.P., and Duffield, J.S. (2010). Fate tracing reveals the pericyte and not epithelial origin of myofibroblasts in kidney fibrosis. Am. J. Pathol. *176*, 85–97.

Indra, A.K., Warot, X., Brocard, J., Bornert, J.M., Xiao, J.H., Chambon, P., and Metzger, D. (1999). Temporally-controlled site-specific mutagenesis in the basal layer of the epidermis: comparison of the recombinase activity of the tamoxifen-inducible Cre-ER(T) and Cre-ER(T2) recombinases. Nucleic Acids Res. *27*, 4324–4327.

Karner, C.M., Das, A., Ma, Z., Self, M., Chen, C., Lum, L., Oliver, G., and Carroll, T.J. (2011). Canonical Wnt9b signaling balances progenitor cell expansion and differentiation during kidney development. Development *138*, 1247–1257.

Kobayashi, A., Shawlot, W., Kania, A., and Behringer, R.R. (2004). Requirement of Lim1 for female reproductive tract development. Development *131*, 539–549.

Kobayashi, A., Kwan, K.M., Carroll, T.J., McMahon, A.P., Mendelsohn, C.L., and Behringer, R.R. (2005). Distinct and sequential tissue-specific activities of the LIM-class homeobox gene Lim1 for tubular morphogenesis during kidney development. Development *132*, 2809–2823.

Kobayashi, A., Valerius, M.T., Mugford, J.W., Carroll, T.J., Self, M., Oliver, G., and McMahon, A.P. (2008). Six2 defines and regulates a multipotent self-renewing nephron progenitor population throughout mammalian kidney development. Cell Stem Cell *3*, 169–181.

Kobayashi, A., Stewart, C.A., Wang, Y., Fujioka, K., Thomas, N.C., Jamin, S.P., and Behringer, R.R. (2011). β-Catenin is essential for Müllerian duct regression during male sexual differentiation. Development *138*, 1967–1975.

Levinson, R., and Mendelsohn, C. (2003). Stromal progenitors are important for patterning epithelial and mesenchymal cell types in the embryonic kidney. Semin. Cell Dev. Biol. *14*, 225–231.

Levinson, R.S., Batourina, E., Choi, C., Vorontchikhina, M., Kitajewski, J., and Mendelsohn, C.L. (2005). Foxd1-dependent signals control cellularity in the renal capsule, a structure required for normal renal development. Development *132*, 529–539.

Lin, E.E., Sequeira-Lopez, M.L., and Gomez, R.A. (2014). RBP-J in FOXD1+ renal stromal progenitors is crucial for the proper development and assembly of the kidney vasculature and glomerular mesangial cells. Am. J. Physiol. Renal Physiol. *306*, F249–F258.

Little, M.H., and McMahon, A.P. (2012). Mammalian kidney development: principles, progress, and projections. Cold Spring Harb. Perspect. Biol. *4*, a008300.

Little, M.H., Brennan, J., Georgas, K., Davies, J.A., Davidson, D.R., Baldock, R.A., Beverdam, A., Bertram, J.F., Capel, B., Chiu, H.S., et al. (2007). A high-resolution anatomical ontology of the developing murine genitourinary tract. Gene Expr. Patterns *7*, 680–699.

Mugford, J.W., Sipilä, P., McMahon, J.A., and McMahon, A.P. (2008). Osr1 expression demarcates a multi-potent population of intermediate mesoderm that undergoes progressive restriction to an Osr1-dependent nephron progenitor compartment within the mammalian kidney. Dev. Biol. *324*, 88–98.

Mugford, J.W., Yu, J., Kobayashi, A., and McMahon, A.P. (2009). High-resolution gene expression analysis of the developing mouse kidney defines novel cellular compartments within the nephron progenitor population. Dev. Biol. *333*, 312–323.

Park, J.S., Valerius, M.T., and McMahon, A.P. (2007). Wnt/beta-catenin signaling regulates nephron induction during mouse kidney development. Development *134*, 2533–2539.

Park, J.S., Ma, W., O'Brien, L.L., Chung, E., Guo, J.J., Cheng, J.G., Valerius, M.T., McMahon, J.A., Wong, W.H., and McMahon, A.P. (2012). Six2 and Wnt regulate self-renewal and commitment of nephron progenitors through shared gene regulatory networks. Dev. Cell *23*, 637–651.

Quaggin, S.E., and Kreidberg, J.A. (2008). Development of the renal glomerulus: good neighbors and good fences. Development *135*, 609–620.

Saxen, L. (1987). Organogenesis of the Kidney (New York: Cambridge University Press).

Schedl, A. (2007). Renal abnormalities and their developmental origin. Nat. Rev. Genet. *8*, 791–802.

Shakya, R., Watanabe, T., and Costantini, F. (2005). The role of GDNF/Ret signaling in ureteric bud cell fate and branching morphogenesis. Dev. Cell *8*, 65–74.

Soriano, P. (1999). Generalized lacZ expression with the ROSA26 Cre reporter strain. Nat. Genet. *21*, 70–71.

Visel, A., Thaller, C., and Eichele, G. (2004). GenePaint.org: an atlas of gene expression patterns in the mouse embryo. Nucleic Acids Res. *32* (Database issue), D552–D556.

Wang, Y., Tripathi, P., Guo, Q., Coussens, M., Ma, L., and Chen, F. (2009). Cre/lox recombination in the lower urinary tract. Genesis *47*, 409–413.

Wiggins, R.C. (2007). The spectrum of podocytopathies: a unifying view of glomerular diseases. Kidney Int. *71*, 1205–1214.

Yu, J., Carroll, T.J., Rajagopal, J., Kobayashi, A., Ren, Q., and McMahon, A.P. (2009). A Wnt7b-dependent pathway regulates the orientation of epithelial cell division and establishes the cortico-medullary axis of the mammalian kidney. Development *136*, 161–171.

Zhang, P., Liégeois, N.J., Wong, C., Finegold, M., Hou, H., Thompson, J.C., Silverman, A., Harper, J.W., DePinho, R.A., and Elledge, S.J. (1997). Altered cell differentiation and proliferation in mice lacking p57KIP2 indicates a role in Beckwith-Wiedemann syndrome. Nature *387*, 151–158.

Stem Cell Reports, Volume *3*

Supplemental Information

Identification of a Multipotent Self-Renewing Stromal Progenitor Population during Mammalian Kidney Organogenesis

Akio Kobayashi, Joshua W. Mugford, A. Michaela Krautzberger, Natalie Naiman, Jessica Liao, and Andrew P. McMahon

SUPPLEMENTAL EXPERIMENTAL PROCEDURES

Mouse strains

Foxd1-Cre knock-in alleles were generated as follows. *Foxd1* targeting vectors were generated with sequence-confirmed homologous arms subcloned by PCR from a BAC clone RPCI23-164L13. The *eGFPCre (GC)*, *CreER^{T2} (CE)*, or *eGFPCreER^{T2} (GCE)* constructs followed by an *FRT-PGKneobpA-FRT* selection cassette (Kobayashi et al., 2008) was introduced into the 5' UTR of the *Foxd1* locus. Mice were generated as previously described (Behringer et al., 2013; Kobayashi et al., 2008). *Foxd1$^{GC/+}$*, *Foxd1$^{CE/+}$*, and *Foxd1$^{GCE/+}$* mouse lines were maintained on 129/Sv x C57BL/6J mixed backgrounds.

Foxd1-Cre alleles were genotyped using the following primers (*Cre*-Fw14; TTGCCTGCATTACCGGTCGATGCAACGAGT, *Cre*-Rv15; CCTGGTCGAAATCAGTGCGTTCGAACGCTA, *mFoxd1*-Fw30; GATCTGCGAGTTCATCAGCAGCCGCTTCCCT, *mFoxd1*-Rv31; GGAAGCTGCCGTTGTCGAACATATCT), which give a 403-bp band for the *Foxd1-Cre* alleles (*Cre*-Fw14 and *Cre*-Rv15) and a 194-bp band for the *Foxd1* wild-type allele (*mFoxd1*-Fw30 and *mFoxd1*-Rv31).

Six2$^{TGC/+}$ mice (Kobayashi et al., 2008) were maintained on 129/Sv x C57BL/6J mixed backgrounds. *R26R-lacZ* Cre reporter (Kobayashi et al., 2008) mice were purchased from Jackson Laboratory and maintained on C57BL/6J x Swiss Webster mixed backgrounds. The mice were genotyped s described previously (Kobayashi et al., 2008).

FACS analysis

FACS analysis of kidney cells was performed as described previously (Kobayashi et al., 2008). Briefly, kidneys from *Foxd1$^{GC/+}$* mice were dissected and treated in 300 µl Trypsin (Invitrogen, 25200-072) at 37 ºC for 3-5 min. After adding 600 µl DMEM media (Invitrogen, 11965) containing 10% sheep serum (Sigma, S2263), a single cell suspension was prepared by pipetting. Cells were collected by centrifugation and resuspended in 100 µl of PBS (Mediatech, 21-031-CV) containing 2% sheep serum. FACS analysis was performed using DAKO Cytomation MoFlo.

Histology

Histology on kidneys was performed as described previously (Kobayashi et al., 2008). Briefly, dissected kidneys were fixed in 4 % paraformaldehyde for 1 hr at 4 ºC and soaked in 30 % sucrose overnight at 4 ºC. After embedding in OCT (Sakura, 4583), cryosections were generated at 16 µm using a Microm HM 550 cryostat.

X-gal staining

X-gal staining was performed as described previously (Kobayashi et al., 2005; Kobayashi et al., 2004). Cryosections were stained with X-gal at 37 ºC overnight and counter-stained with 0.2 % Eosin-Y (Polysciences Inc.). Whole-mount kidneys were fixed in 4 % paraformaldehyde for 1 hr at 4 ºC and stained at 37 ºC overnight for embryonic samples, or at 4 ºC for 2-3 days for neonate samples.

Immunofluorescence

Sections were incubated with primary antibodies against SIX2 (Kobayashi et al., 2008), FOXD1 (Mugford et al., 2008), WT1 (Santa Cruz, sc-192), NPHS1 (Abcam, ab58968), PODXL (R&D Systems, MAB1556), FLK1 (Pharmingen, 555307), PDGFRB (eBiosciences, 14-1402-82), F4/80 (eBioscience, 14-4801), CDKN1C (Abcam, ab4058), LIV2 (MBL International, D118-3), SMA (Sigma, A5228), GFP (Aves labs, GFP-1020; Rockland, 200341-215), β-gal (Cappel, #55976; Abcam, ab9361; Promega, Z3781) and pan-cytokeratin (Sigma, C2562) and detected by the secondary antibodies with DyLight 488, 549 and 649 (Jackson ImmunoResearch Laboratories) or Alexa Fluor 488, 568, 633 and 647 (Invitrogen). Sections were stained with Hoechst (Invitrogen, H3570) prior to mounting with Immu-Mount Medium (Fisher, 9990412). Fluorescent images were photographed on Zeiss LSM510, LSM710 and LSM780 confocal microscopes, and a Nikon Eclipse C1si confocal microscope.

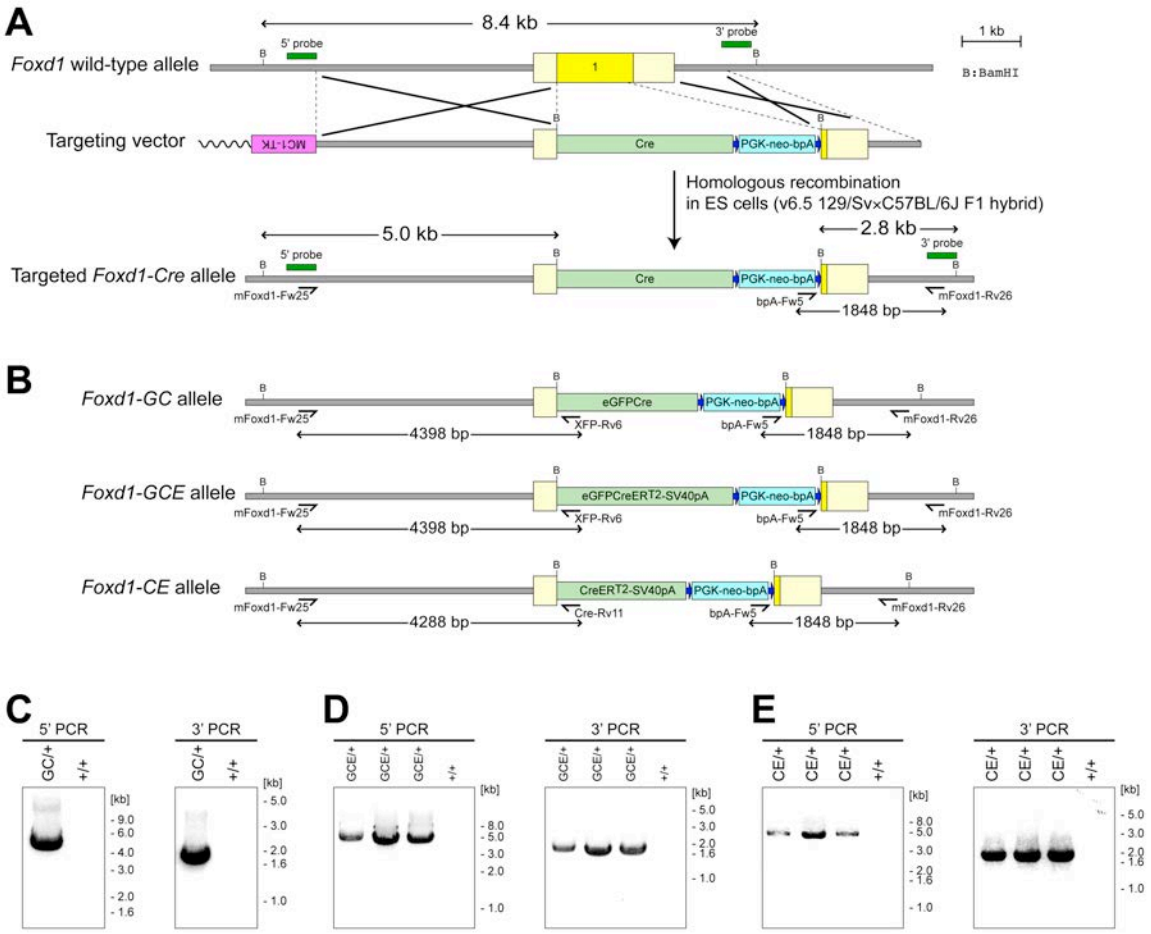

Supplemental Figure 1. Generation of *Foxd1-Cre* knock-in alleles. (A) Schematic illustration of targeting strategy for *Foxd1-Cre* knock-in alleles. **(B)** Targeted *Foxd1-Cre* loci. **(C-E)** Confirmation of targeted *Foxd1-Cre* loci by long-range PCR. (C) *Foxd1-GC*. (D) *Foxd1-GCE*. (E) *Foxd1-CE*. *Foxd1-Cre* alleles were screened using the following primers (bpA-Fw5; GCTGGGGATGCGGTGGGCTCTATGGCTTCT, Cre-Rv11; GGTTCTTGCGAACCTCATCACTCGTTGCAT, mFoxd1-Rv26; CCATCTGCTATAAGCAGGGCTCGCAGTA, mFoxd1-Fw25; CTGTGGGTTGGAATTAGCTCAGCGTTAGGTA, XFP-Rv6; GCACGGGCAGCTTGCCGGTGGTGCAGAT and Cre-Rv11; GGTTCTTGCGAACCTCATCACTCGTTGCAT). Detailed description of the targeting strategy is available upon a request.

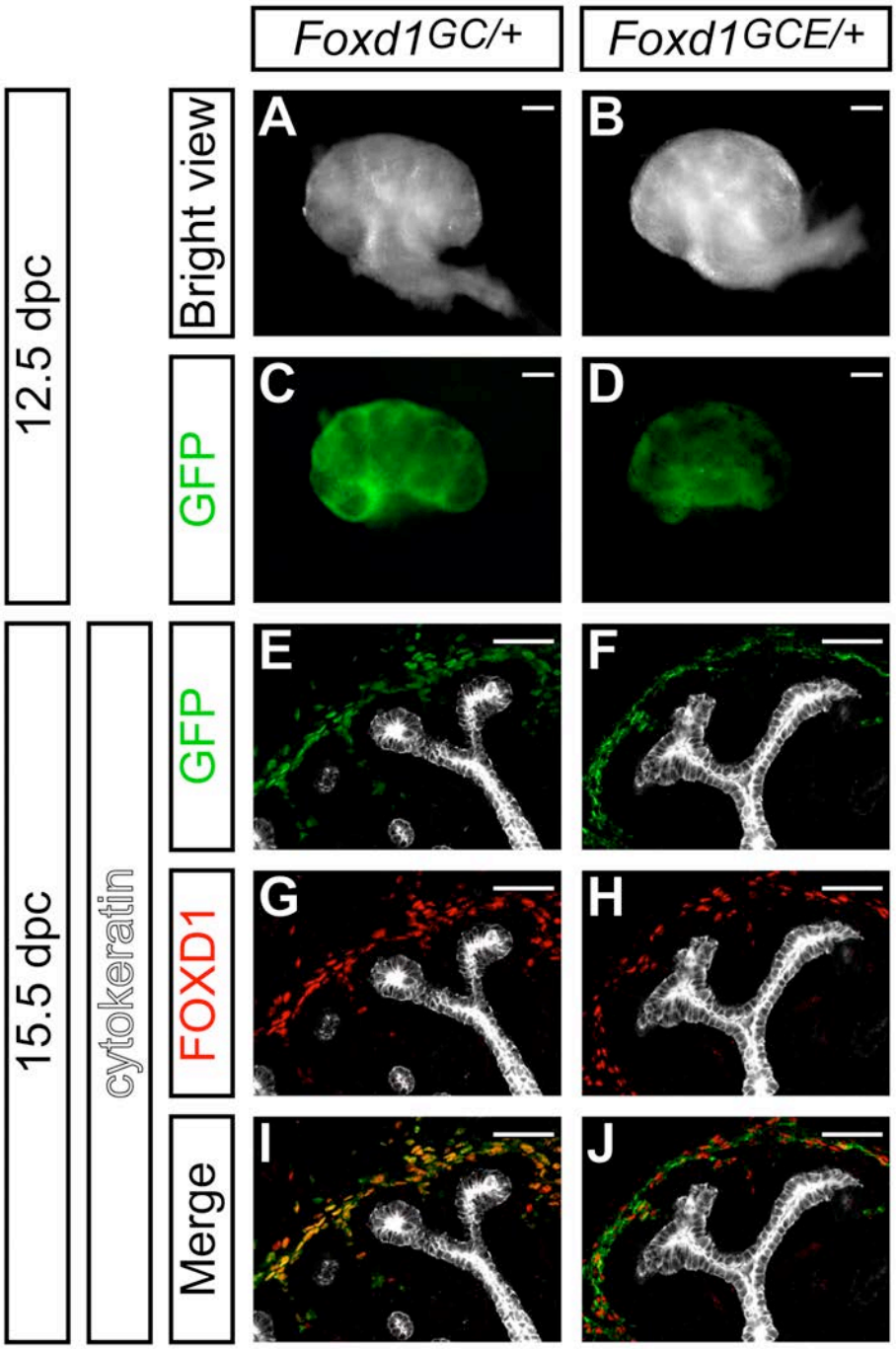

Supplemental Figure 2. *Foxd1-eGFPCre* transgenes are expressed in the FOXD1+ cortical stroma. Kidneys from *Foxd1*$^{GC/+}$ (A,C,E,G,I) and *Foxd1*$^{GCE/+}$ (B,D,F,H,J) knock-in alleles at 12.5 dpc (A-D) and 15.5 dpc (E-J). **(A-D)** Whole-mount kidneys. (A,B) Bright view. (C,D) GFP expression. **(E-J)** Confocal immunofluorescence images of GFP (green), FOXD1 (red) and cytokeratin (KRT, white). At this stage, high levels of cytokeratin are evident in the ureteric tip and collecting duct. Note, the FOXD1 transcriptional regulator localizes in the nucleus, while eGFPCre and eGFPCreER^{T2} proteins show nuclear and cytoplasmic localization, respectively. Scale bars, 100 μm in A-D, 50 μm in E-J.

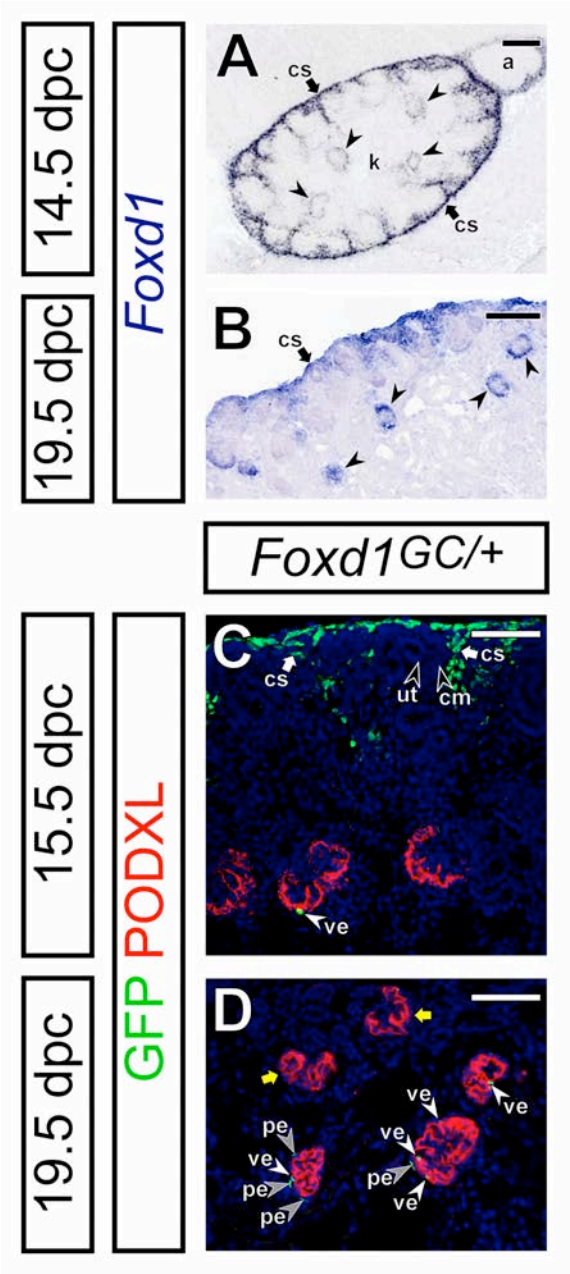

Supplemental Figure 3. The *Foxd1-GFP* is expressed in the visceral and parietal epithelium of the glomerulus. (A,B) *Foxd1* expression in the wild-type kidney by section *in situ* hybridization at 14.5 dpc adapted from the GenePaint database (Visel et al., 2004) and 19.5 dpc adapted from the GUDMAP database (Harding et al., 2011; McMahon et al., 2008). *Foxd1* is expressed in the cortical stroma (cs) and glomerulus (arrowheads). **(C,D)** Confocal immunofluorescence images of *Foxd1*$^{GC/+}$ kidneys at 15.5 dpc (C) and 19.5 dpc (D) with anti-GFP (green), anti-PODXL (Podocalyxin, red) and Hoechst (blue) staining. *Foxd1-GFP* expression was observed in some cells in the both visceral (podocytes) and parietal epithelium of maturing glomeruli, but not in less-differentiated glomeruli (yellow arrows in D). a, adrenal gland; cm, cap mesenchyme; cs, cortical stroma; k, kidney; pe, parietal epithelium; ut, ureteric tip; ve, visceral epithelium (podocytes). Scale bars, 200 μm in A, 100 μm in B, 50 μm in C and D.

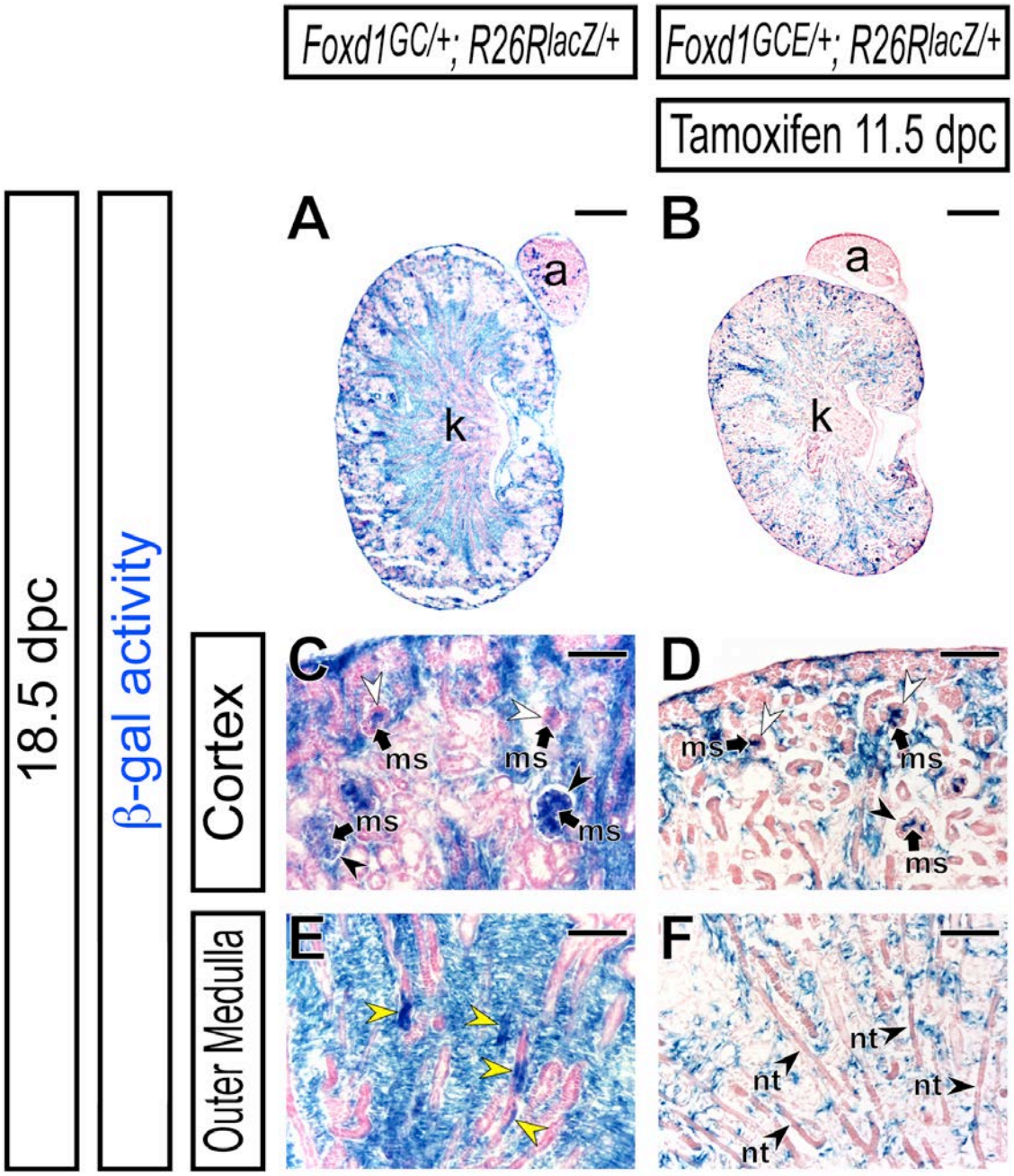

Supplemental Figure 4. A few tubular epithelial cells in some nephrons are derived from the *Foxd1*+ population. X-gal stained (blue) kidneys at 18.5 dpc with eosin counter-staining (pink) from *Foxd1*$^{GC/+}$*; R26R*$^{lacZ/+}$ embryos (A,C,E) and *Foxd1*$^{GCE/+}$*; R26R*$^{lacZ/+}$ embryos with 6 mg tamoxifen injection at 11.5 dpc (B,D,F). **(A,B)** Whole view. **(C-F)** Higher magnification of the renal cortex with glomeruli (C,D) and the outer medulla (E,F). White and black arrowheads in C and D indicate podocytes of glomeruli at less differentiated capillary loop stage stages and maturing stages, respectively. Yellow arrowheads in E indicate β-gal+ cell in the nephron tubule in *Foxd1*$^{GC/+}$*; R26R*$^{lacZ/+}$ kidneys. a, adrenal gland; k, kidney; ms, mesangium; nt, nephron tubule. Scale bars, 500 μm in A and B, 100 μm in C-F.

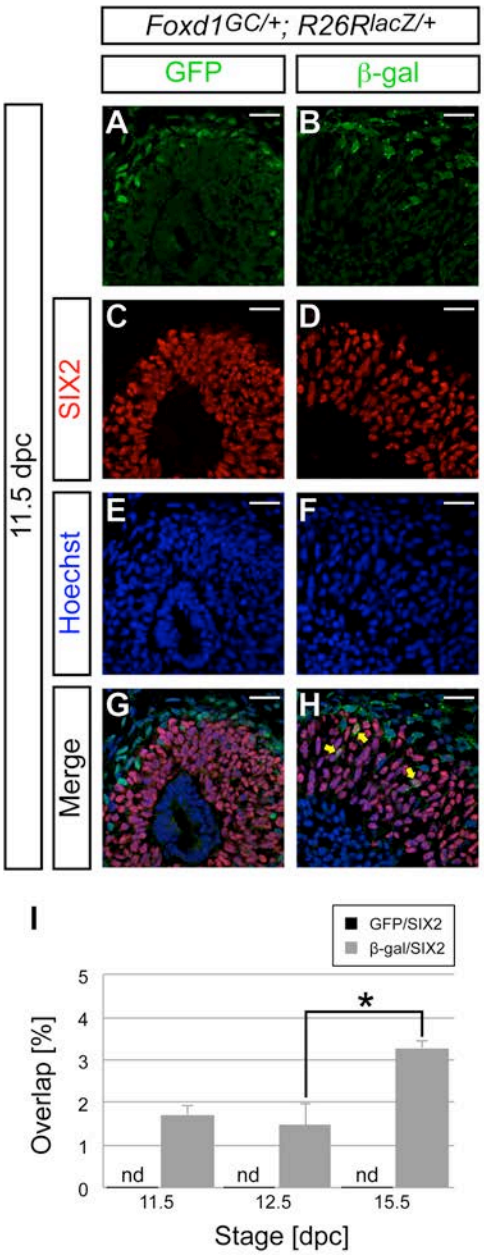

Supplemental Figure 5. *Foxd1*+ cells contribute to a small portion of SIX2+ cap mesenchyme cells. (**A-H**) Confocal immunofluorescence images of the nephrogenic zone of the kidney at 11.5 dpc with anti-GFP (A, green), anti-β-gal (B, green), anti-SIX2 (C,D, red), and Hoechst (E,F, blue) staining and merged images (G,H). Yellow arrows in H indicate β-gal+ SIX2+ cells. Scale bars, 25 μm. (**I**) While no overlap was detected between GFP and SIX2 at 11.5, 12.5, and 15.5 dpc, the frequency of β-gal+ SIX2+ cells in the SIX2+ population significantly increases during development (1.74 ± 0.20, 1.49 ± 0.48, 3.31 ± 0.16 at 11.5, 12.5 and 15.5 dpc, respectively; * $p<0.05$, unpaired t-test) from three biological replicates (n=3) analyzed for each stage. Total numbers of SIX2+ cells counted were 2,389, 1,433 and 1,156 at 11.5, 12.5 and 15.5 dpc, respectively. Data are presented as mean ± SEM (standard error of the mean). nd, not detected. Scale bars, 25 μm.

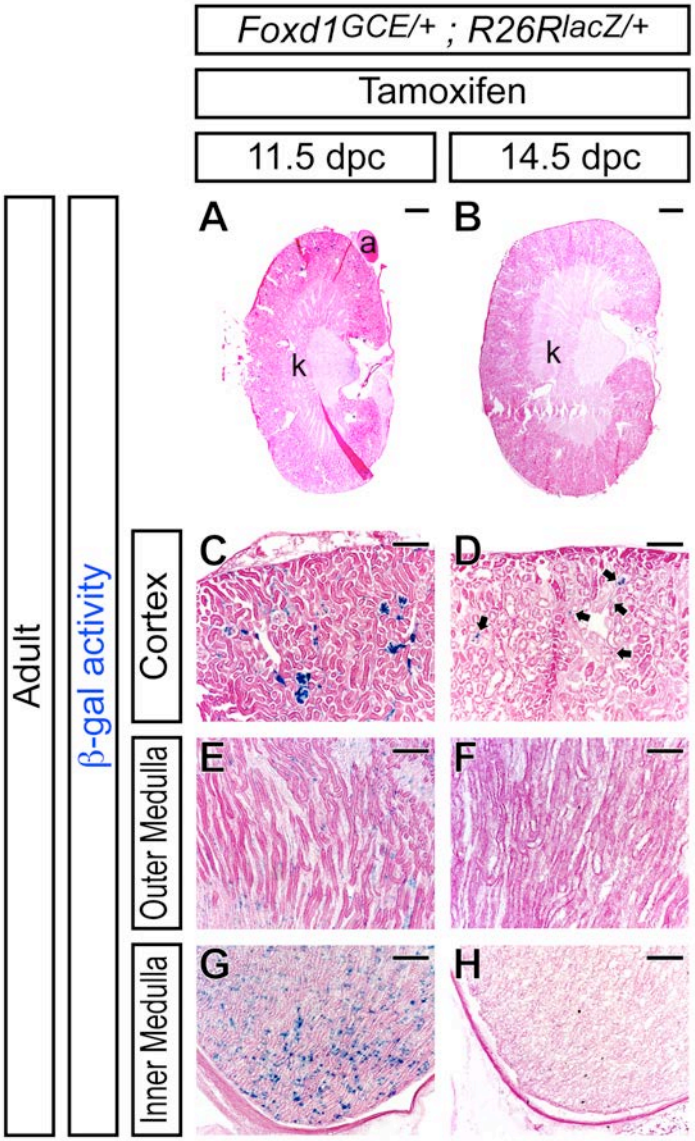

Supplemental Figure 6. The stage-dependent contribution of *Foxd1*+ cortical stromal cells to renal stromal tissues along the cortico-medullary axis is maintained in adult kidneys. X-gal stained (blue) sections counter-stained with eosin (pink) of 6-week old kidneys from *Foxd1*$^{GCE/+}$*; R26R*$^{lacZ/+}$ adult males after injections of 2 mg tamoxifen at 11.5 dpc (A,C,E,G) and 14.5 dpc (B,D,F,H). **(A,B)** Whole kidney. **(C,D)** Renal cortex. **(E,F)** Outer renal medulla. **(G,H)** Inner renal medulla (papilla). Arrows in D indicate β-gal+ cells in the renal cortex. While *Foxd1*+ cortical stromal cells at 11.5 dpc contributed to renal stromal cells in the inner medulla, medulla and cortex (C,E,G), contribution of *Foxd1*+ cortical stromal cells at 14.5 dpc is restricted to the cortex only. Although we observed very rare β-gal+ cells in the inner medulla in kidneys with tamoxifen injection at 14.5 dpc (H and data not shown), our confocal immunofluorescence showed that these rare β-gal+ cells do not express stromal markers including PDGFRB (data not shown). Therefore, it is unlikely that these β-gal+ cells are renal stromal cells, although their identities and origins are currently unclear. a, adrenal gland; k, kidney. Scale bars, 1 mm in A and B, 200 μm in C-H.

REFERENCES

Behringer, R., Gertsenstein, M., Vintersten Nagy, K., Nagy, A., Nagy, K.V., 2013. Manipulating the mouse embryo : A laboratory manual, Fourth edition. ed. Cold Spring Harbor Laboratory Press.

Harding, S.D., Armit, C., Armstrong, J., Brennan, J., Cheng, Y., Haggarty, B., Houghton, D., Lloyd-MacGilp, S., Pi, X., Roochun, Y., Sharghi, M., Tindal, C., McMahon, A.P., Gottesman, B., Little, M.H., Georgas, K., Aronow, B.J., Potter, S.S., Brunskill, E.W., Southard-Smith, E.M., Mendelsohn, C., Baldock, R.A., Davies, J.A., Davidson, D., 2011. The GUDMAP database--an online resource for genitourinary research. Development (Cambridge, England) 138, 2845-2853.

Kobayashi, A., Kwan, K.M., Carroll, T.J., McMahon, A.P., Mendelsohn, C.L., Behringer, R.R., 2005. Distinct and sequential tissue-specific activities of the LIM-class homeobox gene Lim1 for tubular morphogenesis during kidney development. Development (Cambridge, England) 132, 2809-2823.

Kobayashi, A., Shawlot, W., Kania, A., Behringer, R., 2004. Requirement of Lim1 for female reproductive tract development. Development (Cambridge, England) 131, 539-549.

Kobayashi, A., Valerius, M.T., Mugford, J.W., Carroll, T.J., Self, M., Oliver, G., McMahon, A.P., 2008. Six2 defines and regulates a multipotent self-renewing nephron progenitor population throughout mammalian kidney development. Cell stem cell 3, 169-181.

McMahon, A.P., Aronow, B.J., Davidson, D.R., Davies, J.A., Gaido, K.W., Grimmond, S., Lessard, J.L., Little, M.H., Potter, S.S., Wilder, E.L., Zhang, P., 2008. GUDMAP: the genitourinary developmental molecular anatomy project. J Am Soc Nephrol 19, 667-671.

Mugford, J.W., Sipila, P., McMahon, J.A., McMahon, A.P., 2008. Osr1 expression demarcates a multi-potent population of intermediate mesoderm that undergoes progressive restriction to an Osr1-dependent nephron progenitor compartment within the mammalian kidney. Developmental biology 324, 88-98.

Visel, A., Thaller, C., Eichele, G., 2004. GenePaint.org: an atlas of gene expression patterns in the mouse embryo. Nucleic acids research 32, D552-556.